SCIENCE CHINA
Earth Sciences

•RESEARCH PAPER•

July 2020 Vol.63 No.7: 985–998
https://doi.org/10.1007/s11430-019-9582-9

Preliminary analysis of earthquake probability based on the synthetic seismic catalog

Yunqiang SUN[1,2,3], Gang LUO[1*], Caibo HU[2] & Yaolin SHI[2]

[1] *School of Geodesy and Geomatics, Wuhan University, Wuhan 430079, China;*
[2] *Key Laboratory of Computational Geodynamics of Chinese Academy of Sciences, College of Earth and Planetary Sciences, University of Chinese Academy of Sciences, Beijing 100049, China;*
[3] *College of Transportation and Civil Engineering, Fujian Agriculture and Forestry University, Fuzhou 350002, China*

Received May 31, 2019; revised January 4, 2020; accepted February 3, 2020; published online March 27, 2020

Abstract The analysis of seismic hazards relies on the statistical analysis of historical seismic data and the instrumental seismic catalog to obtain the regional earthquake recurrence interval and earthquake probability. The accuracy of analysis thus depends strongly on the completeness of the seismic data used. However, available seismic catalogs are too short or incomplete for the reliable analysis of the statistical characteristics of earthquakes. If a long-term synthetic seismic catalog can be generated using a physics-based numerical simulation, and the simulation results match the crustal deformation, seismicity, and other observations, then such a synthetic catalog helps us to further understand the characteristics of seismic activity and analyze the regional seismic hazard. In this paper, taking the northeastern Tibetan Plateau as a case study, we establish a three-dimensional visco-elasto-plastic finite-element model to simulate earthquake cycles and the spatiotemporal evolution of earthquakes on the model fault system and obtain a seismic catalog on a time scale of tens of thousands of years. On the basis that the model satisfies the regional geodynamics of the northeastern Tibetan Plateau, we analyze seismicity on the northeastern Tibetan Plateau using the simulated synthetic earthquake catalog. The characteristics of earthquake recurrence at different locations and different magnitudes, and the long-term average probability of earthquake occurrence within the fault system on the northeastern Tibetan plateau are studied. The results are a reference for regional seismic hazard assessment and provide a basis for the physics-based numerical prediction of earthquakes.

Keywords Synthetic seismic catalog, Seismic hazard, Recurrence interval of earthquakes, Earthquake probability, Northeastern Tibetan Plateau

Citation: Sun Y, Luo G, Hu C, Shi Y. 2020. Preliminary analysis of earthquake probability based on the synthetic seismic catalog. Science China Earth Sciences, 63: 985–998, https://doi.org/10.1007/s11430-019-9582-9

1. Introduction

Mainland China faces a serious hazard in the form of earthquakes. Earthquakes frequently occur, with great intensity and wide distribution, resulting in severe damage in mainland China (Chen, 2009; Zhang et al., 2013). In the 20th century, nearly half (~590000) of the world's deaths resulting from earthquakes (~1200000) were in China (Zhang et al., 2005; Ma et al., 2007; Chen, 2009). It is, therefore, of great practical and social importance for China to explore and analyze earthquake predictions.

Since the Xingtai earthquake struck in 1966, China has been carrying out large-scale earthquake prediction research in a planned manner (Zhang et al., 2005; Huang et al., 2017; Shi et al., 2018). Most earthquake prediction methods are presently empirical, and this situation is expected to continue for the foreseeable future (Shi et al., 2018). However, for more than half a century, there has been no remarkable

* Corresponding author (email: gangluo66@gmail.com)

breakthrough in the empirical prediction of earthquakes (Shi et al., 2018). Although the 1975 Haicheng earthquake was successfully predicted, there were no advance forecasts of the subsequent Tangshan earthquake in 1976 and the Wenchuan earthquake in 2008. Internationally, the United States, Japan, and other countries have planned programs of earthquake prediction research (Press and Brace, 1966; Hagiwara and Rikitake, 1967) and have explored the use of several observation methods, such as those based on responses of the gravity field (Kisslinger, 1975), geomagnetic field (Rabeh et al., 2009), geoelectricity (Zhao and Qian, 1994), streamflow and water wells (Montgomery and Manga, 2003) and geochemical methods (Grant et al., 2011). However, the difficulties of earthquake prediction were far beyond expectations. In particular, the Parkfield Earthquake Prediction experiment in the United States failed; i.e., scientists predicted that an earthquake would strike around 1988 and by 1993 at the latest, yet the earthquake did not strike until September 28, 2004, at a magnitude of M_w6.0. This failure resulted in the practice of earthquake prediction being questioned for a long time. Some researchers, therefore, hold the view that earthquakes are unpredictable (Geller, 1997; Geller et al., 1997). However, most researchers, including those who believe that earthquakes cannot be predicted deterministically, still insist that earthquakes can be predicted probabilistically. Shi et al. (2018) pointed out that, strictly speaking, natural-science forecasting is always probabilistic forecasting, with deterministic forecasting being the special case that the probability approximates 100%.

Internationally, the earliest and most famous systematic regional earthquake probabilistic model was proposed by the Working Group on California Earthquake Probabilities in the United States (Working Group on California Earthquake Probabilities, 1988) and applied to the San Andreas fault system for probabilistic seismic hazard analysis; the group then developed the Uniform California Earthquake Rupture Forecast (UCERF) system (Field et al., 2014). The UCERF system calculates regional earthquake probabilities for different earthquake magnitudes in a certain time window. This system, to some extent, covers long-term, mid-term and, short-term earthquake probability prediction. Although the UCERF system is the best model for earthquake probability prediction in California, it still has problems. As an example, the number of unknowns in the inversion is much larger than the number of equations (i.e., there are 22000 unknowns versus 2630 equations). There is thus no unique solution for this model; i.e., there are still many subjective factors affecting the quality of the results (Shi et al., 2018). Italy developed the Operational Earthquake Forecast system following the 2009 M_w6.3 Laquila earthquake (Jordan et al., 2011). This system provides a spatial map of the earthquake probability for different earthquake magnitudes in a certain future time window in monitoring areas and provides an earthquake probability forecast continuously updated according to real-time seismic data. Chinese scholars have used a variety of probability models to analyze the earthquake probability in China. As an example, the fifth Generation Seismic Zonation Map of China is currently combined with maps of active faults and potential seismic zones in probabilistic seismic hazard analysis, providing a new means of probabilistic seismic hazard analysis that considers the nonuniform spatial distribution of intraplate earthquakes (Hu, 2001; Gao, 2015). Jiang and Wu (2008) used a predictive model of earthquake physics based on the statistical mechanics of complex systems, namely the Pattern Informatics (PI) model, to estimate the probability of future earthquakes in the Sichuan-Yunnan region and conducted a retrospective forecast test of the PI model using data of earthquakes that had struck since 1988 in the region. They then explored the possibility of applying this model to the estimation of the time-dependent seismic hazard in continental China. Wen (1998) analyzed the time-dependent probability of earthquakes in the Sichuan-Yunnan region. Rong and Jackson (2002) applied a smoothed seismicity method to intraplate regions and estimated the long-term earthquake potential in mainland China. Most of these studies were based on the recorded seismic catalog for prediction of the probability of future earthquakes in a region, and the results thus strongly depended on the timespan and the completeness of seismic magnitude information of the recorded seismic catalog. A more extended and more complete seismic catalog would provide more reliable results of modeling. Therefore, a seismic catalog containing a longer timespan can help us fully understand the characteristics of seismicity, and analyze the earthquake probability and regional seismic hazards. However, available seismic catalogs are mainly based on historical and instrumental records. The accuracies of the locations and magnitudes of historical earthquakes are relatively low, and there are often omissions, especially in sparsely populated areas. Modern instrumental seismic observations have only been developed over the last 100 years. Relative to the recurrence interval of hundreds or even thousands of years for large earthquakes in mainland China, this recording time is too short. Using an instrumental seismic catalog spanning only 100 years or even decades as primary data to calculate earthquake probabilities and analyze regional seismic hazards is obviously not enough. A synthetic long-term seismic catalog can largely make up for the shortcomings (i.e., being too short or incomplete) of an available seismic catalog. It is, therefore, important that we can synthesize a long-term seismic catalog for seismic tectonic research and seismic hazard analysis.

Many studies have investigated the simulation of synthetic seismic catalogs and proposed and developed various models, such as the Burridge-Knopoff model (Burrideg and

Knopoff, 1967), cellular automata model (Wolfram, 1984) and synthetic seismicity simulation models (Ward, 1992; Robinson and Benites, 1996; Ben-Zion et al., 2003; Zhou, 2008). These studies are essential to the theoretical analysis of seismicity and the preliminary analysis of the regional seismic hazard. However, the studies were mainly based on two-dimensional, single-fault models, which are inadequate to use for a real complex multi-fault system. The finite-element method can be adopted to establish a geological model that is closer to reality.

In this study, taking the northeastern Tibetan Plateau as an example, we establish a three-dimensional visco-elasto-plastic finite-element model and simulate earthquake cycles and the spatiotemporal evolution of the earthquake sequence (i.e., the synthetic seismic catalog) on the fault system in this region. We analyze the characteristics of earthquake recurrence and earthquake probability for different magnitudes and different locations along faults, using the synthetic seismic catalog and available earthquake data. The results obtained in this paper provide a reference for seismicity, the characteristics of earthquake recurrence, and an assessment of the long-term seismic hazard in the northeastern Tibetan Plateau and provide a basis for the numerical forecasting of earthquakes based on physical principles.

2. Tectonic background

The northeastern Tibetan Plateau is located at the junction of the Tibet, Ordos, and Alxa blocks (Zhang et al., 1988; Burchfiel et al., 1991); it is one of the most seismically active regions in mainland China (Tapponnier and Molnar, 1977; Zhang et al., 1988) with several active faults, such as Haiyuan fault, Xiangshan-Tianjingshan fault, Helanshan fault, and Luoshan fault (Figure 1). Over the past several hundred years, there have been six major earthquakes with magnitude $M \geq 7$ in this region: the $M\,7\frac{1}{4}$ Luoshan earthquake occurred on the Luoshan fault in 1561; the $M7$ Guyuan North earthquake occurred on the Yunwushan-Xiaoguanshan fault in 1622; the $M7.5$ Zhongwei earthquake occurred on the Xiangshan-Tianjingshan fault in 1709; the $M8$ Pingluo earthquake occurred on the Helanshan fault in 1739; the $M8.5$ Haiyuan earthquake occurred on the Haiyuan fault in 1920; and the $M8$ Gulang earthquake occurred on the Xiangshan-Tianjingshan fault in 1927 (Figure 1). These major earthquakes occurred on major faults in this region (Figure 1). Researchers have carried out a large number of seismic, geological, geophysical studies, etc. in this region (Zhang et al., 1988; Min et al., 2000; Zhang et al., 2005; Liu-Zeng et al., 2007; Wang et al., 2012; Zheng et al., 2013). These fundamental researches provide important constraints for the study of geodynamic numerical simulation.

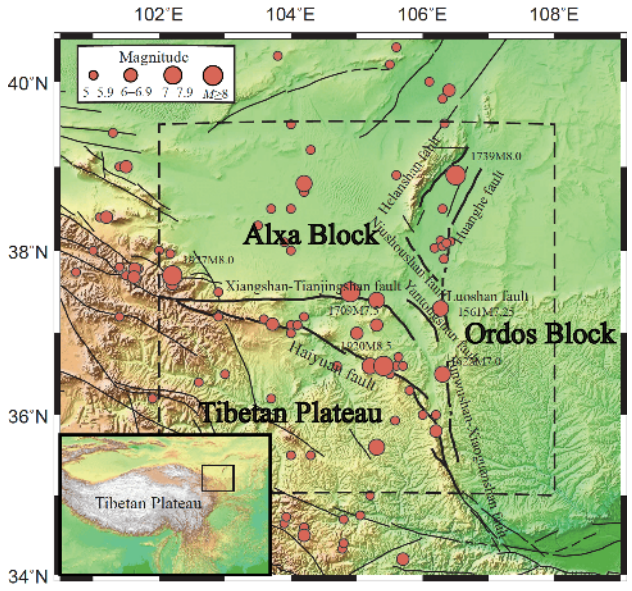

Figure 1 Tectonic background in the northeastern Tibetan Plateau. Red circles show regional historical earthquakes. Earthquake data are taken from the literature (Institute of Geology, China Earthquake Administration and Ningxia Bureau of China Earthquake Administration, 1990).

3. Finite-element model

We set up a three-dimensional finite-element model and simulate earthquake cycles in the northeastern Tibetan Plateau. The basic codes used in this study have been successfully applied in many regions (Luo and Liu, 2010, 2012; Sun and Luo, 2018; Yin et al., 2018; Sun et al., 2019); the reliability of this codes has been verified. We then describe the model setting in the following sections.

3.1 Model setup

Figure 2 shows the finite-element model in the northeastern Tibetan Plateau. The length and width are both 500 km in the model, and the depth is 100 km. The model consists of two rheological layers: a 20 km thick, elasto-plastic upper crust (the faults embedded in the upper crust are simulated by 2 km thick, strain-softening material), and an 80 km thick, visco-elastic lower crust and upper mantle layer.

The setting of the model parameters is based on the results of previous researches. The Young's modulus and Poisson's ratio for the elasto-plastic layer are 8.75×10^{10} Pa and 0.25, respectively. The cohesion and internal frictional angle for the crust of the Tibetan Plateau are 20 MPa and 15°, respectively; while the cohesion and internal frictional angle are 30 MPa and 25° for the crust of the Alxa block and the Ordos block. Since the strength of the fault system is relatively weak, the cohesion and internal frictional angle are set as 10 MPa and 5°, respectively (Turcotte and Schubert, 1982; Li et al., 2009; Luo and Liu, 2010; Sun and Luo, 2018). The Young's modulus and Poisson's ratio for the lower crust and

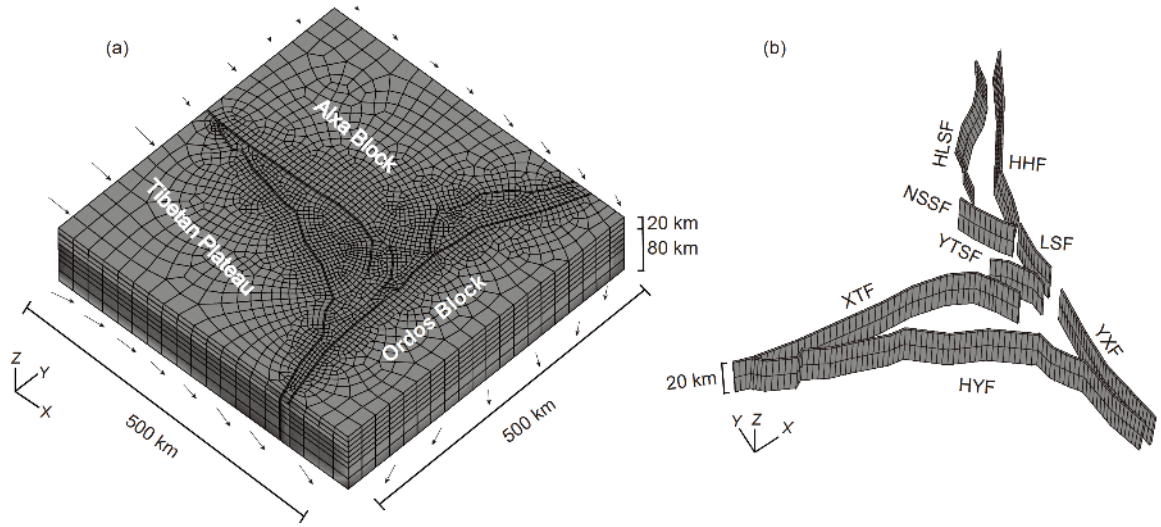

Figure 2 Finite-element model and fault system in the model. (a) Mesh and boundary conditions of the model for the northeastern Tibetan Plateau. Lateral boundary conditions are determined by the interpolation of Global Positioning System data (Gan et al., 2007). (b) Fault system in the model. HLSF, Helanshan fault; HHF, Huanghe fault; LSF, Luoshan fault; NSSF, Niushoushan fault; YTSF, Yantongshan fault; XTF, Xiangshan-tianjingshan fault; YXF, Yunwushan-xiaoguanshan fault; HYF, Haiyuan fault.

upper mantle layer are 8.75×10^{10} Pa and 0.25, respectively (Turcotte and Schubert, 1982; Luo and Liu, 2010; Sun and Luo, 2018). The viscosity for the lower crust and upper mantle of the Tibetan Plateau is 1×10^{20} Pa·s, while the value is 1×10^{23} Pa·s for the lower crust and upper mantle of the Ordos block and the Alxa block (Zang et al., 2005; Xiao and He, 2015).

In this study, we use the GPS data (Gan et al., 2007) which revealed the velocity field relative to the stable Eurasian plate during 1998–2004, and interpolate the velocity field to the lateral boundaries in our model. We use the velocities multiply the loading time steps as the displacement boundary conditions in the model. We assume the lateral boundary conditions of the model do not change with depth, and this is also used in many other studies (Luo and Liu, 2010; Zhu and Zhang, 2013; Xiao and He, 2015; Pang et al., 2019). The upper surface is set for free, and the bottom surface can move freely horizontally but fixed vertically.

3.2 Governing equations

The model simulates lithospheric deformation by solving the static equation of force equilibrium:

$$\frac{\partial \boldsymbol{\sigma}_{ij}}{\partial x_j}+f_i=0, \tag{1}$$

where $\boldsymbol{\sigma}_{ij}$ is stress tensor (i, j=1, 2, 3), f_i is body force.

Our model calculates strain increments in each time step; and the strain increment consists of viscous, elastic, and plastic components:

$$\{\mathrm{d}\varepsilon\} = \{\mathrm{d}\varepsilon^{v}\} + \{\mathrm{d}\varepsilon^{e}\} + \{\mathrm{d}\varepsilon^{p}\}, \tag{2}$$

where $\{\mathrm{d}\varepsilon^{v}\}$, $\{\mathrm{d}\varepsilon^{e}\}$ and $\{\mathrm{d}\varepsilon^{p}\}$ represent viscous strain component, elastic strain component, and plastic strain component, respectively. {} represents a tensor.

The model follows the Maxwell linear visco-elastic deformation when the stresses do not reach the yield strength. The visco-elastic constitutive relation can be written as:

$$\begin{aligned}\{\mathrm{d}\varepsilon^{v}\} &= [\mathbf{Q}]^{-1}\{\boldsymbol{\sigma}^{t}\}\mathrm{d}t = [\mathbf{Q}]^{-1}(\{\boldsymbol{\sigma}^{t-\mathrm{d}t}\} + \{\mathrm{d}\sigma\})\mathrm{d}t,\\ \{\mathrm{d}\varepsilon^{e}\} &= [\mathbf{D}]^{-1}\{\mathrm{d}\sigma\},\end{aligned} \tag{3}$$

where $\{\boldsymbol{\sigma}^{t}\}$ is the stress tensor at model time t, dt is the time increment, $\{\mathrm{d}\sigma\}$ is the increment stress tensor, [**D**] and [**Q**] represent the elastic and viscous material matrices, respectively.

When the model stresses reach the yield strength, the plastic deformation occurs.

The Drucker-Prager yield criterion is used:

$$\begin{aligned}F(\sigma, C) &= \sqrt{\mathbf{J}_2} - \alpha\mathbf{I}_1 - \beta,\\ \alpha &= \frac{2\sin\varphi}{\sqrt{3}(3+\sin\varphi)},\\ \beta &= \frac{6C\cos\varphi}{\sqrt{3}(3+\sin\varphi)},\end{aligned} \tag{4}$$

where $\mathbf{I}_1$ is the first invariant of stress tensor, $\mathbf{J}_2$ is the second invariant of deviatoric stress tensor, α and β are parameters of the Drucker-Prager criterion that related to cohesion (C) and internal frictional angle (φ).

Since the plastic shear strain increment of the model material is much larger than the plastic volume strain increment, the non-associated flow law is adopted (Chen, 2007; Sun and Luo, 2018). The plastic strain increment can be written as:

$$\{\mathrm{d}\varepsilon^{p}\} = \mathrm{d}\lambda\left\{\frac{\partial G}{\partial \sigma}\right\}, \tag{5}$$

where $d\lambda$ is the plastic multiplier.

Three-dimensional visco-elasto-plastic constitutive relation is given as:

$$\{d\sigma\} = \left([\tilde{\mathbf{D}}] - [\mathbf{D}_p]\right)\{d\varepsilon\} + \{d\tilde{\sigma}\} - \{d\tilde{\sigma}_p\}. \quad (6)$$

More details can be found in (Li et al., 2009; Luo and Liu, 2010; Sun and Luo, 2018).

3.3 Simulating earthquake cycles

We used the Drucker-Prager yield criterion to determine whether there is an earthquake that occurred in the model. When stresses on the fault elements do not reach the yield strength ($F(\sigma, C)<0$), the model stays within the interseismic tectonic loading states (Figure 3). With continuous tectonic loading, stresses increase; when the stresses reach the yield strength ($F(\sigma, C)=0$), we decrease the cohesion on fault elements (the cohesion drops ΔC on faults are estimated from the coseismic stress drop (Kanamori and Anderson, 1975) on each fault, where, Haiyuan fault: 6.2×10^6 Pa, Yunwushan-Xiaoguanshan fault: 4×10^6 Pa, Xiangshan-Tianjingshan fault: 5×10^6 Pa, Helanshan fault: 7×10^6 Pa, Luoshan fault: 5.8×10^6 Pa, Huanghe fault: 3.2×10^6 Pa, Yantongshan fault: 5.8×10^6 Pa, and Niushoushan fault: 5×10^6 Pa). A sudden decrease of cohesion will cause instability in the model, and thus, causing the coseismic slip. Namely, an earthquake occurs; at the same time, we set the time step to be 1 s. The stresses state at this moment shows $F(\sigma, C-\Delta C)>0$. Due to the release of coseismic stress, the instability stresses state will change; stresses on fault elements will decrease. Until the residual stresses on fault elements satisfy the weakened yield strength ($F(\sigma, C-\Delta C)=0$), the earthquake ends (Figure 3). We can calculate the moment magnitude for each earthquake in the model according to the areas of failure elements and coseismic slips. Generally, a fault element yield represents a small earthquake; multiple elements yield represents a big earthquake. A big earthquake usually takes several hundred seconds to complete. After an earthquake ends, the cohesion of the yield elements immediately returns from $C-\Delta C$ to C. The model enters the postseismic viscoelastic stress relaxation period and the interseismic loading period toward the next earthquake. This process can be repeated, so we simulate the earthquake cycles (Figure 3) (Luo and Liu, 2010, 2018; Sun and Luo, 2018; Sun et al., 2019).

4. Model results

4.1 Background stress

Initial stress conditions are important in geodynamic numerical simulation (Zhu and Zhang, 2013; Zhu et al., 2015), yet the initial conditions are difficult to determine and constrain owing to the complexity and inaccessibility of the earth (Chen, 2009).

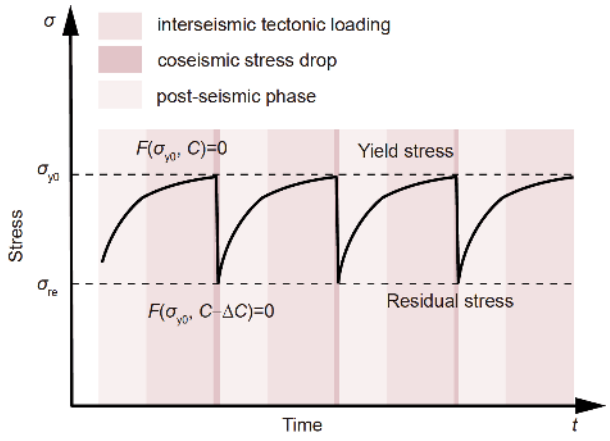

Figure 3 Sketch showing stress accumulation and stress release during earthquake cycles.

The stress states of the earth's crust mainly include the tectonic loading state, co-seismic stress release state, and postseismic stress acceleration state. These states occur on the basis of the background stress field during earthquake cycles. Stress changes relating to these three stages are small compared with the background stress. As an example, the average background stress or tectonic shear stress of the upper crust is generally several dozen megapascals, while the average shear stress change due to an earthquake is several megapascals or even smaller (Kanamori and Anderson, 1975).

The initial stress state in our modeling is a lithostatic stress state (Luo and Liu, 2010; Sun and Luo, 2018). With continued tectonic loading, the stress accumulates and reaches a steady-state in a model time of about 50000 years. This steady-state is the background stress state in our modeling; we calculate and analyze the model results using this background stress field. The results show that the modeled interseismic velocity field after the model reaches the steady-state is comparable to the velocity field acquired by the Global Positioning System (Sun and Luo, 2018); and the modeled stress state is consistent with that revealed by regional earthquake mechanisms (Sun et al., 2019). The model results and observation data compare well, indicating that the model reveals the geodynamic background (Shi et al., 2018) in the northeastern Tibetan Plateau. We thus keep the model running and get the synthetic seismic catalog for this region (Figure 4).

4.2 Synthetic seismic catalog

We simulate earthquake cycles and the spatiotemporal evolution of the earthquake sequence and synthesize the long-term (on the scale of tens of thousands of years) seismic catalog (Figure 4) using the modeled background stress field for the northeastern Tibetan Plateau.

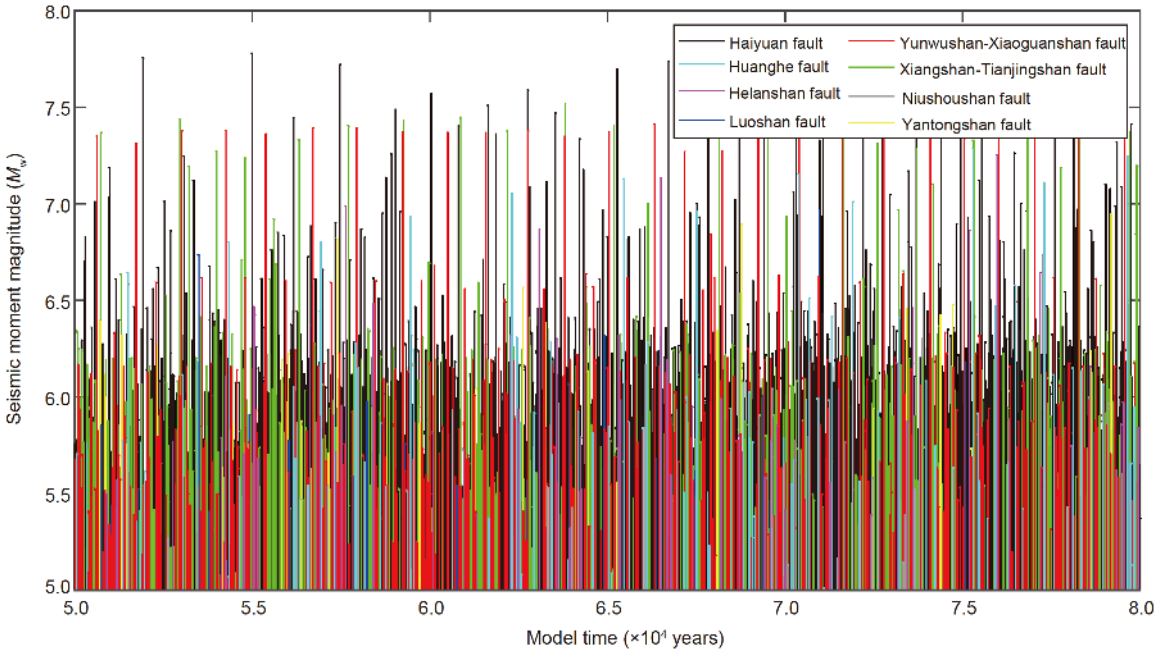

Figure 4 Synthetic seismic catalog on the fault system of the northeastern Tibetan Plateau.

We calculate the relation between the earthquake magnitude and earthquake frequency using this synthetic seismic catalog to test whether this synthetic catalog satisfies the *G-R* relation. The *G-R* relation is one of the most important statistical relations of seismicity (Gutenberg and Richter, 1944), indicating a negative linear correlation between the seismic magnitude and the cumulative number of earthquakes (Gutenberg and Richter, 1944; Wiemer and Wyss, 2000; Schorlemmer and Wiemer, 2005; Parsons, 2007). The *G-R* relation can, therefore, be used as an important criterion in testing whether a synthetic seismic catalog is correct, complete, and reasonable. Figure 5 shows the magnitude-frequency distribution of the synthetic seismic catalog. The results show that the synthetic seismic catalog satisfies the *G-R* relation when the earthquake magnitude $M_w \geq 5.5$ (i.e., the complete magnitude M_c is 5.5), and the *b*-value is 1.01 (Figure 5a). We also calculate the regional *b*-value using the instrumental seismic catalog for 2008–2017 provided by the China Seismic Network Center; results show that M_c=1.2 and *b*=0.96 (Figure 5b). We find that the *b*-value calculated using our synthetic seismic catalog is consistent with the value obtained using the instrumental seismic catalog; the values are also near the global-average *b*-value (1.0) (Nuannin et al., 2005; El-Isa and Eaton, 2014). We thus assume that our synthetic seismic catalog reflects seismicity in the northeastern Tibetan Plateau.

4.3 Characteristics of earthquake recurrence on the model fault system

We synthesized the long-term (on the order of tens of thousands of years) seismic catalog for the northeastern Tibetan Plateau (Figure 4). We can also calculate the synthetic seismic catalog for each fault in the model (Figure 6). According to the synthetic seismic catalog for each fault, we initially estimate the average recurrence interval of earthquakes with different magnitudes for each fault in the model. Table 1 gives the average recurrence interval of earthquakes with $M_w \geq 6.0$ and $M_w \geq 7.0$ for regional faults. Model results show that the average recurrence interval of earthquakes (both $M_w \geq 6.0$ and $M_w \geq 7.0$) is shortest for the Haiyuan fault; i.e., the recurrence interval of earthquakes is 32 years for $M_w \geq 6.0$ and 309 years for $M_w \geq 7.0$. The recurrence interval of earthquakes is the longest (2858 years) for the Niushoushan fault when with $M_w \geq 6.0$. There are no earthquakes with $M_w \geq 7.0$ for some individual faults in the model, e.g., the Luoshan fault. The maximum magnitude of earthquakes is M_w6.9 for the Luoshan fault in our modeling. However, paleoearthquake studies and historical earthquake records show that there have been earthquakes with magnitude greater than 7 along this fault (The Research Group on Active Fault System around Ordos Massif, 1988; Min et al., 2000). According to the empirical magnitude conversion relation (M_w=(1.06±0.08)M−(0.58±0.60)) (Chen, 2017), the moment magnitude of M_w6.7 is close to M7. We thus also calculate the recurrence interval of earthquakes with $M_w \geq 6.7$ on the Luoshan fault in the model (2500 years); this result is comparable to that of M7 earthquakes (2300–2700 years) obtained in paleoearthquake studies (Min et al., 2000). We find that the initially estimated recurrence intervals of earthquakes with $M_w \geq 7.0$ on the Haiyuan fault and Xiangshan-Tianjingshan fault (Table 1, Haiyuan fault: 309 years;

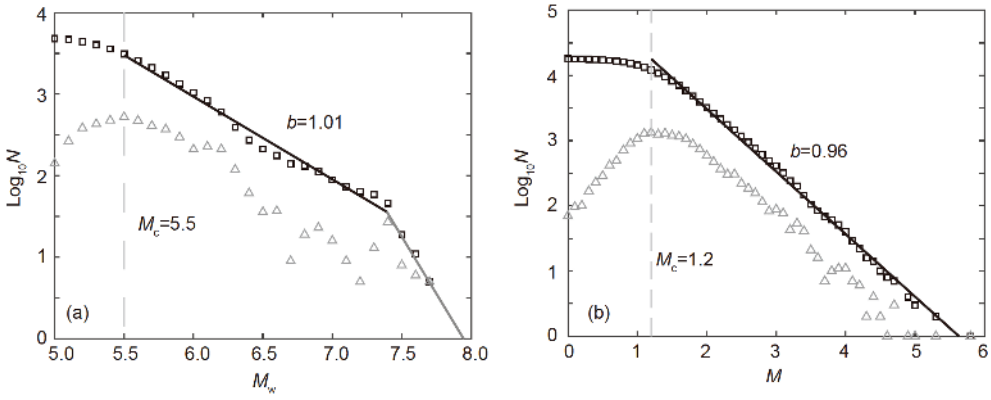

Figure 5 Earthquake magnitude-frequency distribution. (a) Earthquake magnitude-frequency distribution from the synthetic seismic catalog; (b) earthquake magnitude-frequency distribution from the instrumental record seismic catalog. The triangles and squares show the noncumulative and cumulative magnitude-frequency distributions, respectively.

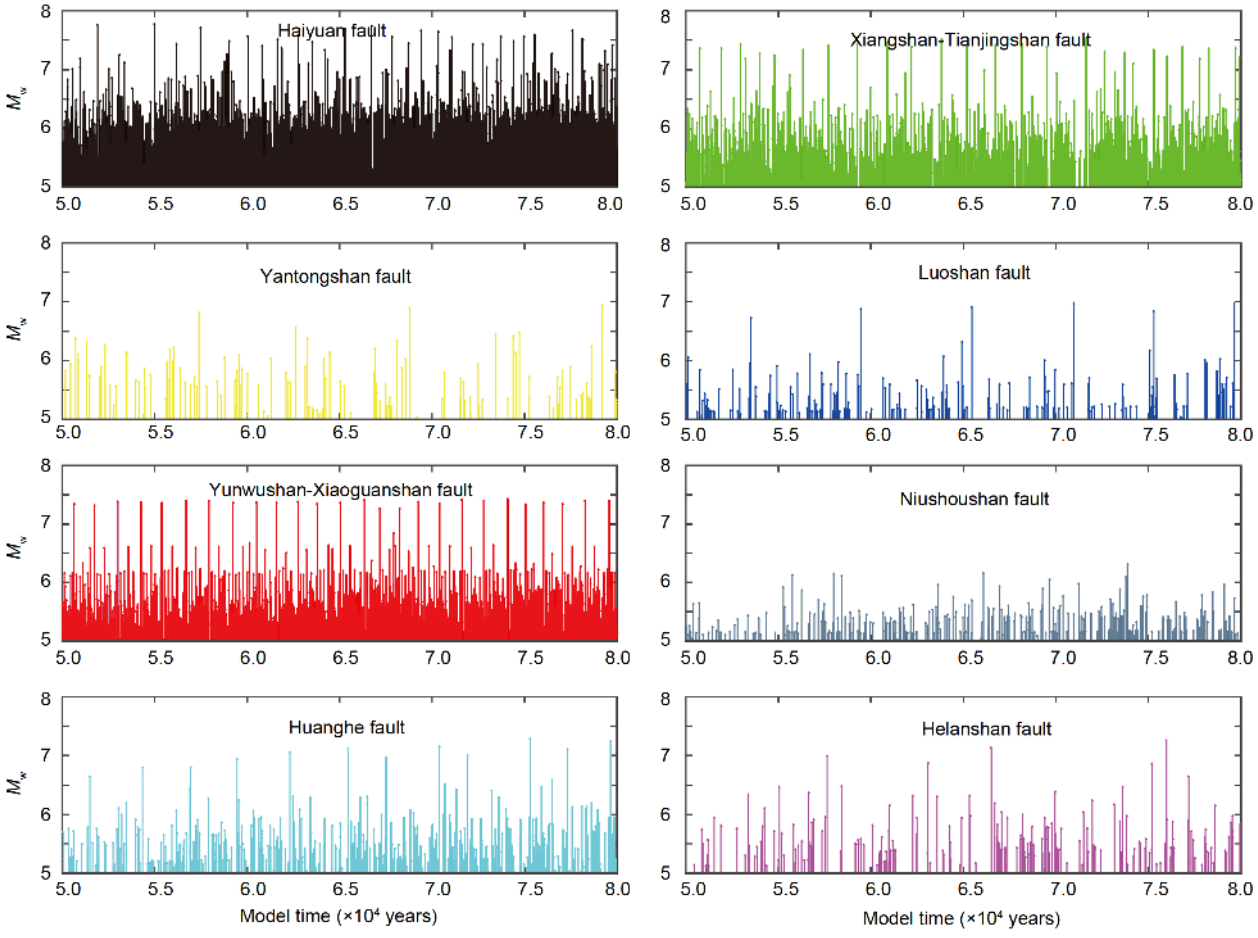

Figure 6 Synthetic seismic catalog on different faults in the model.

Xiangshan-Tianjingshan fault: 612 years) are shorter than the intervals obtained in previous paleoearthquake studies (Haiyuan fault: ~500–2500 years; Xiangshan-Tianjingshan fault: ~2000 years (Institute of Geology, China Earthquake Administration and Ningxia Bureau of China Earthquake Administration, 1990; Min et al., 2000; Zhang et al., 2005)). This is because we treat each fault zone as a whole when we estimate the recurrence interval of earthquakes. Here, the recurrence interval of earthquakes on each fault is defined as the ratio of the statistical model time to the number of earthquakes with $M_w \geq 6.0$ or $M_w \geq 7.0$ on each fault. However, the seismicity of the Haiyuan fault and Xiangshan-Tianjingshan fault is segmented along the fault strike (Zhang et al., 2005; Zheng et al., 2013; Sun et al., 2019). In our

Table 1 Average recurrence interval of earthquakes on faults in the model

Fault	Recurrence interval of earthquakes (year)			References
	Model results	Paleoearthquake results		
	M_w≥6.0	M_w≥7.0	M≥7.0	
Haiyuan fault	32	309	500–2500	Institute of Geology, China Earthquake Administration and Ningxia Bureau of China Earthquake Administration (1990); Zhang et al. (2005); Min et al. (2000); Liu-Zeng et al. (2007); Liu et al. (1992)
Xiangshan-Tianjingshan fault	89	612	2000	Zhang et al. (2005); Min et al. (2000)
Yantongshan fault	1250	–	–	
Luoshan fault	1819	–	2300–2700	Zhang et al. (2005); The Research Group on Active Fault System around Ordos Massif (1988)
Yunwushan-Xiaoguanshan fault	159	1112	–	
Niushoushan fault	2858	–	–	
Huanghe fault	572	2500	1500–2000	Lin et al. (2015)
Helanshan fault	870	6667	2300–3000	Lin et al. (2015); Deng and Liao (1996)

model, the fault elements do not always fail together but have a certain segmentation when an earthquake occurs (Sun and Luo, 2018); even the seismicity on different fault segments of the same fault is not evenly distributed. Therefore, for a fault zone with obvious segmentation of seismicity, large errors may occur when using the seismicity of the whole fault zone and its related period to estimate the recurrence interval of earthquakes, as shown in Table 1.

Therefore, we also calculate seismicity at different locations along each fault in the model and obtain the average recurrence interval of earthquakes of different magnitudes at different locations on each fault. Figure 7 shows the recurrence interval (Figure 7a) of earthquakes with M_w≥6.0 and its standard deviation (Figure 7b) and the recurrence interval (Figure 7c) of earthquakes with M_w≥7.0 and its standard deviation (Figure 7d). Results show that the earthquake recurrence is uneven in the modeling; i.e., values for different faults or at different locations along the same faults are remarkably different (Figure 7). The recurrence interval of earthquakes with M_w≥6.0 in the middle segment of the Haiyuan fault is 300–1000 years with a standard deviation of about 100–300 years; the recurrence interval of earthquakes with M_w≥7.0 on this fault segment is 900–1200 years with a standard deviation of about 500 years. The recurrence interval of earthquakes at both ends of the Haiyuan fault (both M_w≥6.0 and M_w≥6.0) is around 2000–3500 years, or even larger (Figure 7). The Haiyuan fault is the most crucial fault of the northeastern Tibetan Plateau, and seismicity on this fault is the most frequent in the regional fault system. Researchers have carried out many seismic and geological studies on this fault (Liu et al., 1992; Min et al., 2000; Zhang et al., 2005; Liu-Zeng et al., 2007). They found that the recurrence interval of earthquakes with M≥7.0 is 500–2500 years on the Haiyuan fault (Liu et al., 1992; Min et al., 2000; Zhang et al., 2005; Liu-Zeng et al., 2007); this result is consistent with our modeling results (Figure 7). Currently, the Maomaoshan-Laohushan fault in the western segment of the Haiyuan fault does not have a record of big earthquakes; i.e., there is a seismic gap (Gaudemer et al., 1995). Therefore, this fault segment is more likely to have a major earthquake in the future. Seismicity along the Xiangshan-Tianjingshan fault shows that the recurrence interval of earthquakes with M_w≥6.0 is about 1000 years (Figure 7a) with a standard deviation of 300–500 years (Figure 7b) while the recurrence interval of earthquakes with M_w≥7.0 is about 1500 years at most locations along this fault (Figure 7c) with a standard deviation of about 400 years (Figure 7d); the exceptions are isolated locations at which the interval is greater than 3000 years. Paleoearthquake studies on the Xiangshan-Tianjingshan fault found that the recurrence interval of earthquakes is about 2000 years (Wang et al., 1990; Min et al., 2000). The recurrence interval of earthquakes with M_w≥7.0 is nearly 1500 years, with a standard deviation of 200 years, on the Yunwushan-Xiaoguanshan fault. There has been less research on the Yunwushan-Xiaoguanshan fault, resulting in fewer seismic records (Institute of Geology, China Earthquake Administration and Ningxia Bureau of China Earthquake Administration, 1990). However, this fault is likely to have a major earthquake because an M7 earthquake has occurred on this fault (i.e., the M7 Guyuan North earthquake that struck in 1622). The number and magnitudes of earthquakes on the Yunwushan-Xiaoguanshan fault in our modeling are more and larger than those obtained in previous research (Institute of Geology, China Earthquake Administration and Ningxia Bureau of China Earthquake Administration, 1990) because we connect the different fault segments seen at the surface into one fault zone (Figure 2). In addition, we set the dip angle of the Yunwushan-Xiaoguanshan fault to be constant (70°) in our modeling. The dip angle of a fault may change with depth in reality, affecting the seismicity. The recurrence interval of earthquakes on the faults where seismicity does not show obvious segmentation

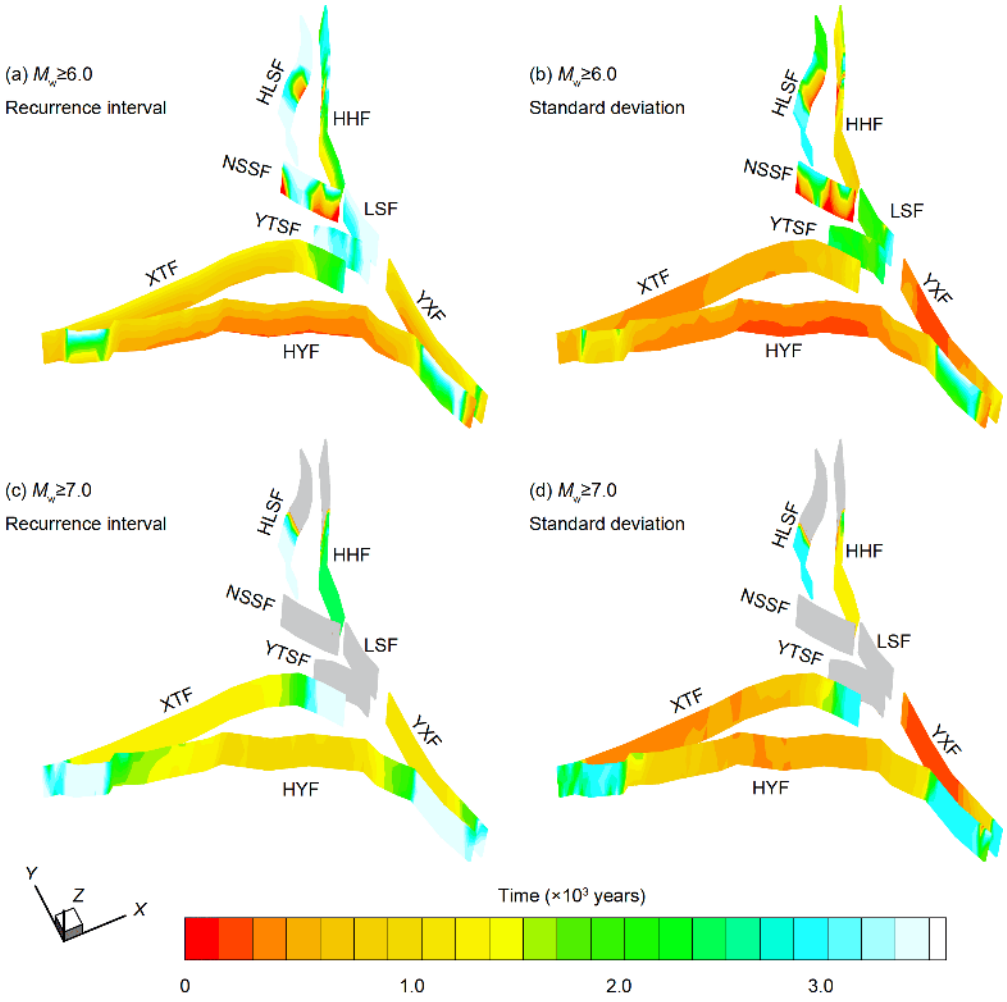

Figure 7 Recurrence interval of earthquakes and the standard deviation. (a) Recurrence interval of earthquakes with magnitude M_w≥6.0; (b) the standard deviation; (c) recurrence interval of earthquakes with magnitude M_w≥7.0; (d) the standard deviation. The gray color indicates that there is no related earthquake in the region.

in the modeling is basically approximate to the results given in Table 1. The recurrence interval of earthquakes with M_w≥6.0 on the Helanshan fault is about 3000 years, the maximum interval is 6667 years (Table 1), and the standard deviation is 1000–3000 years (Figure 7b, 7d). The recurrence interval of earthquakes with M_w≥6.0 on the Huanghe fault is 1000–2500 years (Figure 7a), with a standard deviation of about 700–1500 years (Figure 7b). The recurrence interval of earthquakes with M_w≥7.0 on the Huanghe fault is about 2300 years (Figure 7c) with a standard deviation of about 1200 years (Figure 7d). The recurrence interval of earthquakes with M_w≥6.0 on the Luoshan fault, Yantongshan fault, and Niushoushan fault is 2500–3000 years (Figure 7a) with a standard deviation of about 1500–2000 years (Figure 7d). Our modeling results show that seismicity on the Luoshan fault, Yantongshan fault, and Niushoushan fault is relatively weak, which is consistent with results obtained by previous studies (Institute of Geology, China Earthquake Administration and Ningxia Bureau of China Earthquake Administration, 1990).

We also calculate the variation coefficient of earthquake recurrence for different magnitudes at different locations along each fault in the model. The variation coefficient σ is defined as:

$$\sigma=\frac{T_{\mathrm{std}}}{T_{\mathrm{av}}}, \tag{7}$$

where T_{av} and T_{std} respectively represent the average and standard deviation of the recurrence interval of earthquakes (Kagan and Jackson, 1991; Yi et al., 2002). Earthquake clusters while the variation coefficient greater than 1.0; earthquake recurrence is an entirely random Poisson process while the variation coefficient equals to 1.0; and the earthquake recurrence is quasi-periodic while the variation coefficient less than 1.0 (Yi et al., 2002). It is usually believed that a variation coefficient less than 0.5 well represents the quasi-periodic behavior of earthquake recurrence (Yi et al., 2002).

Figure 8 shows the variation coefficient of earthquake recurrence for M_w≥6.0 (Figure 8a) and M_w≥7.0 (Figure 8b) on the fault system in the modeling. The variation coefficient of earthquake recurrence is uneven in the modeling; the values for different faults or for different locations along the same faults are remarkably different (Figure 8). The variation coefficients of earthquake recurrence for M_w≥6.0 mostly range 0.5–1.0 in the modeling; i.e., the recurrence of earthquakes with M_w≥6.0 shows weak quasi-periodic behavior (Figure 8a). The variation coefficient of earthquake recurrence for M_w≥7.0 is around 1.0 along the Helanshan fault (Figure 8b), which means earthquakes with M_w≥7.0 do not have quasi-periodicity on the Helanshan fault but rather a particular random behavior. Except in a small region where the variation coefficients are greater than 1.0, the variation coefficients along the Yunwushan-Xiaoguanshan fault, Xiangshan-Tianjingshan fault, and Haiyuan fault are mostly around 0.5 (Figure 8b). This means that earthquake recurrence with M_w≥7.0 at most locations along these faults has quasi-periodicity, and this quasi-periodicity is stronger than that of earthquake recurrence for M_w≥6.0 (Figure 8).

4.4 Earthquake probability on model fault system

The genesis of an earthquake is complex, while the time required for earthquake genesis in mainland China is relatively long. In addition, it is difficult to predict earthquakes with certainty at present owing to the numerous shortcomings of observation technologies. Probabilistic seismic hazard analysis is, therefore, the main method of earthquake prediction adopted in seismic science research.

The available seismic catalog is relatively short, and many hypothetical probabilistic distribution models have, therefore, been proposed for mathematical convenience (e.g., Hagiwara, 1974; Utsu, 1984). However, earthquakes do not always satisfy the assumptions of the models; i.e., the observed seismicity tends to be complex. Our model results also show that earthquake recurrence does not strictly obey a Poisson distribution but instead shows complexity; i.e., earthquakes at different locations along a fault system exhibit both quasi-periodicity (for which the variation coefficient of earthquake recurrence is less than 1.0) and clustering (for which the variation coefficient of earthquake recurrence is greater than 1.0) (Figure 8). We therefore directly analyze the synthetic long-term seismic catalog and then calculate the probability of earthquakes in the region. This probability is calculated without making any assumptions about the distribution of earthquake recurrence.

We calculate the long-term average probability of earthquakes striking at different locations of the fault system (i.e., along the fault direction and with depth) using the synthetic seismic catalog for a model time of 20000 years. In this paper, the earthquake probability is defined as the ratio of the number of earthquakes above an absolute magnitude to the number of earthquakes in the model at a fault position during a specific period. Figure 9 shows the probability of earthquakes with M_w≥6.0 (Figure 9a) and M_w≥7.0 (Figure 9b) along with the fault system in the modeling. The earthquake probability is heterogeneous on different faults (Figure 9). For earthquakes with M_w≥6.0, the probability of recurrence is a maximum on the middle segment of the Haiyuan fault, while the probability on the deep fault is greater than that on the shallow fault (i.e., the highest probability of earthquakes is on the location of the fault depth of about 20 km); the

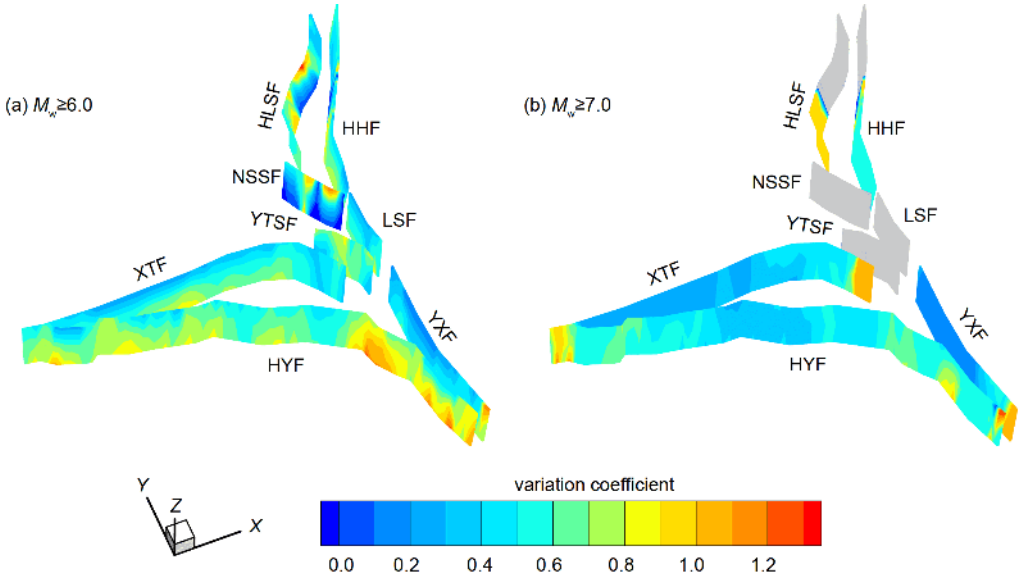

Figure 8 Variation coefficients of earthquake recurrence in the modeling. (a) Variation coefficients of earthquake recurrence for magnitude M_w≥6.0; (b) variation coefficients of earthquake recurrence for magnitude M_w≥7.0. The gray color means there is no related earthquake in the region.

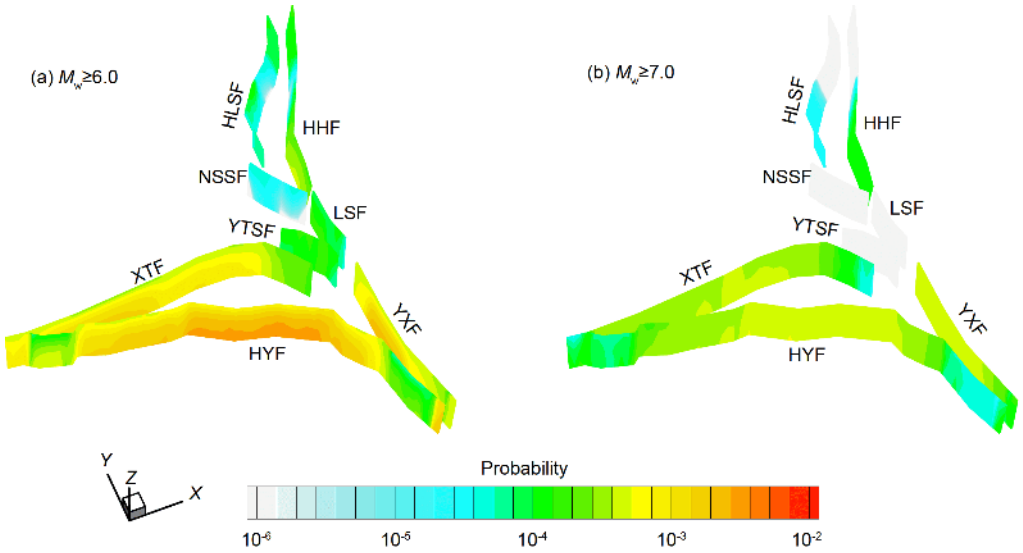

Figure 9 Long-term average probability of earthquake recurrence in the modeling. (a) Probability of earthquake recurrence for magnitude M_w≥6.0; (b) probability of earthquake recurrence for magnitude M_w≥7.0.

maximum probability of earthquakes with M_w≥6.0 can be as high as 0.6% (Figure 9a). The probabilities of earthquakes on the Yunwushan-Xiaoguanshan fault and Xiangshan-Tianjingshan fault respectively reach 0.4% and 0.2%. The probabilities of earthquakes on the Helanshan fault, Huanghe fault, Luoshan fault, Yantongshan fault, and Niushoushan fault are low compared with those on the Haiyuan fault, Yunwushan-Xiaoguanshan fault, and Xiangshan-Tianjingshan fault; the value is basically around 0.01%, or even less (Figure 9a). Among the faults, the probability of earthquake occurrence is lowest on the Niushoushan fault (about 0.005%) in the model fault system, and some locations along the fault do not even have earthquakes with M_w≥6.0.

The spatial distribution of earthquakes with M_w≥7.0 is similar to that of earthquakes with M_w≥6.0 in the modeling; i.e., the probability of earthquake recurrence in the middle segment of the Haiyuan fault is relatively high as a whole (Figure 9b). In general, the number of earthquakes with a certain magnitude is 8–10 times the number of earthquakes with a magnitude one level greater, within a certain period in a region (Chen, 2009). We see that the probability of earthquakes with M_w≥7.0 (0.06%) is lower than that of earthquakes with M_w≥6.0 (0.6%). Results show that the probability of earthquake recurrence is a maximum in the middle segment of the Haiyuan fault (Figure 9). We note that the probability of earthquake recurrence calculated here is a long-term average probability, which is independent of historical earthquakes. According to elastic rebound theory, after a major earthquake occurs in a fault zone, the region enters a stage of stress accumulation, which is relatively safe. As an example, the 1920 *M*8.5 Haiyuan earthquake struck in the middle segment of the Haiyuan fault, and the probability of the next major earthquake occurring in the middle segment of the Haiyuan fault is then lower than that for any other fault segment. The results thus provide a reference for the assessment of a long-term seismic hazard in a region.

5. Discussion

The earthquake recurrence interval and earthquake probability are basic references used in seismic hazard analysis, while the seismic catalog is basic data of the recurrence interval and earthquake probability. However, the available seismic catalogs are too short or incomplete for reliable analysis of the statistical characteristics of earthquakes. In this study, we developed and constructed a three-dimensional visco-elasto-plastic finite-element model for the northeastern Tibetan Plateau. We simulated earthquake cycles and the spatiotemporal evolution of earthquakes and obtained a synthetic seismic catalog on a time scale of tens of thousands of years for the northeastern Tibetan Plateau. We also calculated seismicity at different locations within the model fault system. By analyzing seismicity at different locations within the model fault system, we obtained the recurrence interval of earthquakes and the probability of earthquakes at each location within the fault system (i.e., the tendency along the fault direction). The results obtained in the present study can help us further understand the characteristics of earthquake recurrence and earthquake probability and analyze the regional seismic hazard.

We found that earthquake recurrence within the fault system of the northeastern Tibetan Plateau is complex; i.e., earthquake recurrence on faults exhibits both quasi-periodicity and clustering. It is difficult to accurately predict seismicity in the region according to the characteristics of

earthquake recurrence. Probabilistic seismic hazard analysis is a main means of earthquake prediction. We also calculated the long-term average probability of earthquakes striking in the northeastern Tibetan Plateau. The results show that the probability is a maximum for the middle segment of the Haiyuan fault, followed by the Yunwushan-Xiaoguanshan fault and Xiangshan-Tianjingshan fault. We emphasize that our calculated earthquake probability is the long-term average earthquake probability, which is independent of historical earthquakes. Shi et al. (2018) suggested that the numerical prediction system of earthquakes in China should comprise long-term time-independent earthquake probabilistic forecasting, mid-term time-dependent earthquake probabilistic forecasting, and short-term earthquake probabilistic forecasting. The earthquake probability calculated in this paper is part of the long-term earthquake probabilistic forecasting of this numerical prediction system for earthquakes.

In the compilation of the seismic hazard map of China, the earthquake activity modeling makes three basic assumptions: the earthquake magnitude distribution in a seismic area satisfies the truncated *G-R* relation, earthquakes obey a Poisson distribution, and earthquakes in potential seismic zones are evenly distributed (Pan et al., 2013). We can get the annual average probability of earthquake occurrence by interpolating from the statistical results of the *G-R* relation for small- and medium-sized earthquakes. However, for earthquakes of larger magnitude, the magnitude-frequency distribution often deviates from the linear *G-R* relation of small- and medium-sized earthquakes (Figure 5a) (Cornell, 1968; Wesnousky, 1994; Kagan, 2002). That is to say, the statistical relations of large earthquakes and small- and medium-sized earthquakes may differ and exhibit different patterns, and the annual probability of earthquakes estimated only using the truncated *G-R* relation may have errors (Wyss, 2015). Additionally, our model results show that earthquake recurrence is uneven and does not simply follow a Poisson distribution. In this study, we directly analyzed the synthetic seismic catalog and calculated the long-term average probability of earthquakes, and the calculation did not make any assumptions about the distribution of earthquake recurrence.

Previous studies simulated the seismic cycle according to the rate and state friction law (e.g., van Dinther et al., 2013; Zilio et al., 2018). However, owing to difficulties in implementing numerical methods, most studies adopted two-dimensional single-fault models and thus could not explore the characteristics of seismicity for complex three-dimensional fault systems. In reality, earthquakes occur within complex three-dimensional fault systems. In this study, we used a stress drop model to simulate earthquakes, allowing the simulation of seismic cycles for complex three-dimensional fault systems. This modeling helps us further analyze seismicity within regional multi-fault systems.

Previous research suggests that the Jingtai segment of the Haiyuan fault zone is currently in a creeping state (Cavalié et al., 2008); its impact on regional seismicity remains unclear. The Haiyuan fault was treated as a stick-slip fault in this paper. Additionally, the modeling in this study made many approximations and simplifications. At the same time, owing to parameter uncertainty, it is not enough to calculate and analyze the model results for only one case. Shi et al. (2018) pointed out that we can make calculations for many cases having a reasonable range of parameters, thus obtaining a series of results. The results can be moderately weighted to obtain a comprehensive probability of earthquakes, which is more reliable. The present paper presents preliminary results. These results are a reference for the seismicity of a regional fault system, the characteristics of earthquake recurrence, and the assessment of the long-term seismic hazard and provide a basis for the numerical prediction of earthquakes based on physical principles. The results thus promote the further development of physical-based seismic numerical prediction in China.

6. Conclusions

We analyzed the regional characteristics of earthquake recurrence and the probability of earthquakes using a synthetic seismic catalog for the northeastern Tibetan Plateau and available seismic data for this region. The main conclusions of this study are as follows.

(1) The numerical model developed in this study is a new tool for simulation of regional seismic catalog of a complex fault system. Available seismic catalogs are too short or incomplete, and the synthetic seismic catalog thus helps us better understand the characteristics of seismicity and analyze the regional seismic hazard.

(2) Earthquake recurrence on the fault system of the northeastern Tibetan Plateau shows quasi-periodic behavior as a whole, but this quasi-periodicity is not strong in that there is often a large deviation. It is, therefore, difficult to accurately predict the regional seismicity according to the characteristics of earthquake recurrence.

(3) Seismicity within the fault system of the northeastern Tibetan Plateau is uneven in that earthquake recurrence is different for different faults and different segments of the same fault.

(4) The modeled long-term average probability of earthquakes is a maximum on the middle segment of the Haiyuan fault (where the probability of earthquakes with $M_w \geq 6.0$ reaches 0.6% and the probability of earthquakes with $M_w \geq 7.0$ reaches 0.06%), followed by the Yunwushan-Xiaoguanshan fault and Xiangshan-Tianjingshan fault.

(5) The results of this paper provide a reference for the seismicity of a regional fault system, the characteristics of

earthquake recurrence, and the assessment of the long-term seismic hazard, and provide a basis for the numerical forecasting of earthquakes based on physical principles.

Acknowledgements *We thank three anonymous reviewers for the constructive suggestions. This work was supported by China Earthquake Science Experiment Project, CEA (Grant No. 2019CSES0112), and National Natural Science Foundation of China (Grant Nos. 41574085, 41974107, 41590865 & U1839207).*

References

Ben-Zion Y, Eneva M, Liu Y. 2003. Large earthquake cycles and intermittent criticality on heterogeneous faults due to evolving stress and seismicity. J Geophys Res, 108: ESE4–1

Burchfiel B C, Zhang P Z, Wang Y P, Zhang W Q, Song F M, Deng Q D, Molnar P, Royden L. 1991. Geology of the Haiyuan fault zone, Ningxia-Hui Autonomous region, China, and its relation to the evolution of the northeastern margin of the Tibetan Plateau. Tectonics, 10: 1091–1110

Burrideg R, Knopoff L. 1967. Model and theoretical seismicity. Bull Seismol Soc Amer, 57: 341–371

Cavalié O, Lasserre C, Doin M P, Peltzer G, Sun J, Xu X, Shen Z K. 2008. Measurement of interseismic strain across the Haiyuan fault (Gansu, China), by InSAR. Earth Planet Sci Lett, 275: 246–257

Chen J. 2017. Seismic hazard modeling of the Sichuan-Yunnan region. Dissertation for Doctoral Degree. Beijing: Institute of Geology, China Earthquake Administration. 1–135

Chen M X. 2007. Elasticity and Plasticity (in Chinese). Beijing: Science Press

Chen Y T. 2009. Earthquake prediction: Retrospect and prospect (in Chinese). Sci China Ser D-Earth Sci, 1633–1658

Cornell C A. 1968. Engineering seismic risk analysis. Bull Seismol Soc Amer, 58: 1583–1606

Deng Q D, Liao Y H. 1996. Paleoseismology along the range-front fault of Helan Mountains, north central China. J Geophys Res, 101: 5873–5893

El-Isa Z H, Eaton D W. 2014. Spatiotemporal variations in the *b*-value of earthquake magnitude-frequency distributions: Classification and causes. Tectonophysics, 615-616: 1–11

Field E H, Arrowsmith R J, Biasi G P, Bird P, Dawson T E, Felzer K R, Jackson D D, Johnson K M, Jordan T H, Madden C, Michael A J, Milner K R, Page M T, Parsons T, Powers P M, Shaw B E, Thatcher W R, Weldon R J, Zeng Y. 2014. Uniform California earthquake rupture forecast, Version 3 (UCERF3)—The time-independent model. Bull Seismol Soc Amer, 104: 1122–1180

Gan W J, Zhang P Z, Shen Z K, Niu Z J, Wang M, Wan Y G, Zhou D M, Cheng J. 2007. Present-day crustal motion within the Tibetan Plateau inferred from GPS measurements. J Geophys Res, 112: B08416

Gao M T. 2015. GB18306-2015 "The Ground Motion Parameter Zoing Map of China" Promote and Implement the Teaching Material (in Chinese). Beijing: Standards Press of China

Gaudemer Y, Tapponnier P, Meyer B, Peltzer G, Guo S M, Chen Z T, Dai H G, Cifuentes I. 1995. Partitioning of crustal slip between linked, active faults in the eastern Qilian Shan, and evidence for a major seismic gap, the 'Tianzhu gap', on the western Haiyuan Fault, Gansu (China). Geophys J Int, 120: 599–645

Geller R J. 1997. Earthquake prediction: A critical review. Geophys J Int, 131: 425–450

Geller R J, Jackson D D, Kagan Y Y, Mulargia F. 1997. Earthquakes cannot be predicted. Science, 275: 1616

Grant R A, Halliday T, Balderer W P, Leuenberger F, Newcomer M, Cyr G, Freund F T. 2011. Ground water chemistry changes before major earthquakes and possible effects on animals. Int J Environ Res Public Health, 8: 1936–1956

Gutenberg B, Richter C F. 1944. Frequency of earthquakes in California. Bull Seismol Soc Amer, 34: 185–188

Hagiwara T, Rikitake T. 1967. Japanese Program on Earthquake Prediction: A prediction program now under way in Japan succeeds in long-range forecast of the Matsushiro earthquakes. Science, 157: 761–768

Hagiwara Y. 1974. Probability of earthquake occurrence as obtained from a Weibull distribution analysis of crustal strain. Tectonophysics, 23: 313–318

Hu Y X. 2001. GB18306-2001 "The Ground Motion Parameter Zoing Map of China" Promote and Implement the Teaching Material (in Chinese). Beijing: Standards Press of China

Huang F Q, Zhang X D, Cao Z X, Li J P, Li S H. 2017. The roadmap of numerical earthquake prediction in China (in Chinese). Rec Dev World Seismol, (4): 3–10

Institute of Geology, China Earthquake Administration and Ningxia Bureau of China Earthquake Administration. 1990. Active Haiyuan Fault Zone Monopraph, Special Publications on Active Fault Studies in China (in Chinese). Beijing: Seismological Press

Jiang C S, Wu Z L. 2008. Retrospective forecasting test of a statistical physics model for earthquakes in Sichuan-Yunnan region. Sci China Ser D-Earth Sci, 51: 1401–1410

Jordan T H, Chen Y T, Gasparini P, Madariage R, Main I, Marzocchi W, Papadopoulos G. 2011. Operational earthquake forecasting-state of knowledge and guidelines for utilization. Ann Geophys, 54: 351–391

Kagan Y Y. 2002. Seismic moment distribution revisited: I. Statistical results. Geophys J Int, 148: 520–541

Kagan Y Y, Jackson D D. 1991. Seismic gap hypothesis: Ten years after. J Geophys Res, 96: 21419–21431

Kanamori H, Anderson D L. 1975. Theoretical basis of some empirical relations in seismology. Bull Seismol Soc Amer, 65: 1073–1095

Kisslinger C. 1975. Processes during the Matsushiro, Japan, earthquake swarm as revealed by leveling, gravity, and spring-flow observations. Geology, 3: 57–62

Li Q S, Liu M, Zhang H. 2009. A 3-D viscoelastoplastic model for simulating long-term slip on non-planar faults. Geophys J Int, 176: 293–306

Lin A M, Hu J M, Gong W B. 2015. Active normal faulting and the seismogenic fault of the 1739 M~8.0 Pingluo earthquake in the intracontinental Yinchuan Graben, China. J Asian Earth Sci, 114: 155–173

Liu B C, Yuan D Y, He W G, Liu X F. 1992. Risk analysis of strong earthquakes in west end of Haiyuan fault (in Chinese). Northwestern Seismol J, Suppl: 49–56

Liu-Zeng J, Klinger Y, Xu X W, Lasserre C, Chen G, Chen W, Tapponnier P, Zhang B. 2007. Millennial recurrence of large earthquakes on the Haiyuan fault near Songshan, Gansu Province, China. Bull Seismol Soc Amer, 97: 14–34

Luo G, Liu M. 2010. Stress evolution and fault interactions before and after the 2008 Great Wenchuan earthquake. Tectonophysics, 491: 127–140

Luo G, Liu M. 2012. Multi-timescale mechanical coupling between the San Jacinto fault and the San Andreas fault, southern California. Lithosphere, 4: 221–229

Luo G, Liu M. 2018. Stressing rates and seismicity on the major faults in eastern Tibetan Plateau. J Geophys Res-Solid Earth, 123: 10968–10986

Ma Z J, Gao Q H, Chen J Y, Gao X L. 2007. Development of cause of disaster reduction and integrated reduction of disasters. J Nat Disaster, 16: 1–6

Min W, Zhang P Z, Deng Q D. 2000. Primary study on regional paleoearthquake recurrence behavior (in Chinese). Acta Seismol Sin, 22: 163–170

Montgomery D R, Manga M. 2003. Streamflow and water well responses to earthquakes. Science, 300: 2047–2049

Nuannin P, Kulhanek O, Persson L. 2005. Spatial and temporal *b* value anomalies preceding the devastating off coast of NW Sumatra earthquake of December 26, 2004. Geophys Res Lett, 32: L11307

Pan H, Gao M T, Xie F R. 2013. The earthquake activity model and seismicity parameters in the new seismic hazard map of China (in Chinese). Technol Earthq Disaster Prevention, 8: 11–23

Pang Y J, Cheng H H, Zhang H, Shi Y L. 2019. Numerical analysis of the influence of lithospheric structure on surface vertical movements in Eastern Tibet (in Chinese). Chin J Geophys, 62: 1256–1267
Parsons T. 2007. Forecast experiment: Do temporal and spatial *b* value variations along the Calaveras fault portend $M \geq 4.0$ earthquakes? J Geophys Res, 112: B03308
Press F, Brace W F. 1966. Earthquake prediction. Science, 152: 1575–1584
Rabeh T, Miranda M, Hvozdara M. 2009. Strong earthquakes associated with high amplitude daily geomagnetic variations. Nat Hazards, 53: 561–574
Robinson R, Benites R. 1996. Synthetic seismicity models for the Wellington Region, New Zealand: Implications for the temporal distribution of large events. J Geophys Res, 101: 27833–27844
Rong Y, Jackson D D. 2002. Earthquake potential in and around China: Estimated from past earthquakes. Geophys Res Lett, 29: 27-1–27-4
Schorlemmer D, Wiemer S. 2005. Earth science: Microseismicity data forecast rupture area. Nature, 434: 1086
Shi Y L, Sun Y Q, Luo G, Dong P Y, Zhang H. 2018. Roadmap for earthquake numerical forecasting in China—Reflection on the tenth anniversary of Wenchuan earthquake (in Chinese). Chin Sci Bull, 63: 1865–1881
Sun Y Q, Luo G. 2018. Spatial-temporal migraton of earthquakes in the northeastern Tibetan Plateau: Insights from a finite element model (in Chinese). Chin J Geophys, 61: 2246–2264
Sun Y Q, Luo G, Yin L, Shi Y L. 2019. Migration probability of big earthquakes and segmentation of slip rates on the fault system in northeastern Tibetan Plateau (in Chinese). Chin J Geophys, 62: 1663–679
Tapponnier P, Molnar P. 1977. Active faulting and tectonics in China. J Geophys Res, 82: 2905–2930
The Research Group on Active Fault System around Ordos Massif, SSB. 1988. Active Fault System Around Ordos Massif (in Chinese). Beijing: Seismological Press
Turcotte D L, Schubert G. 1982. Geodynamics: Applications of Continuum Physics to Geological Problems. New York: John Wiley & Sons. 450
Utsu T. 1984. Estimation of parameters for recurrence models of earthquakes. Bull Earthquake Res Inst, Univ Tokyo, 59: 53–66
van Dinther Y, Gerya T V, Dalguer L A, Mai P M, Morra G, Giardini D. 2013. The seismic cycle at subduction thrusts: Insights from seismo-thermo-mechanical models. J Geophys Res-Solid Earth, 118: 6183–6202
Wang H Y, Gao R, Yin A, Xiong X S, Kuang C Y, Li W H, Huang W Y. 2012. Deep structure geometry features of Haiyuan fault and deformation of the crust revealed by deep seismic reflection profiling (in Chinese). Chin J Geophys, 55: 3902–3909
Wang Y P, Song F M, Li Z Y, You H C, An P. 1990. Study on recurrence intervals of great earthquakes in the late Quaternary of Xiangshan-Tianjingshan fault zone in Ningxia (in Chinese). Earthquake Res Chin, 6: 15–24
Ward S N. 1992. An application of synthetic seismicity in earthquake statistics: The Middle America Trench. J Geophys Res, 97: 6675–6682
Wen X Z. 1998. Assessment of time-dependent seismic hazards on segments of active fault, and its problems (in Chinese). Chin Sci Bull, 43: 1457–1466
Wesnousky S G. 1994. The Gutenberg-Richter or characteristic earthquake distribution, which is it? Bull Seismol Soc Amer, 84: 1940–1959
Wiemer S, Wyss M. 2000. Minimum magnitude of completeness in earthquake catalogs: Examples from Alaska, the Western United States, and Japan. Bull Seismol Soc Amer, 90: 859–869
Wolfram S. 1984. Cellular automata as models of complexity. Nature, 311: 419–424
Working Group on California Earthquake Probabilities. 1988. Probabilites of large earthquakes occurring in California on the San Andereas fault. U S Geol Surv, Open-File Report
Wyss M. 2015. Testing the basic assumption for probabilistic seismic-hazard assessment: 11 failures. Seismol Res Lett, 86: 1405–1411
Xiao J, He J. 2015. 3D finite-element modeling of earthquake interaction and stress accumulation on main active faults around the northeastern Tibetan Plateau edge in the past ~100 years. Bull Seismol Soc Amer, 105: 2724–2735
Yi G X, Wen X Z, Xu X W. 2002. Study on recurrence behaviors of strong earthquakes for several entireties of active fault zones in Sichuan-Yunnan region (in Chinese). Earthq Res Chin, 18: 267–276
Yin L, Luo G, Sun Y Q. 2018. Middle-lower crust flow and crustal deformation: Insights from a finite element modeling (in Chinese). Chin J Geophys, 61: 3933–3950
Zang S X, Qiang Wei R, Liu Y G. 2005. Three-dimensional rheological structure of the lithosphere in the Ordos block and its adjacent area. Geophys J Int, 163: 339–356
Zhang G M, Zhang X D, Wu R H, Jiang Z S, Liu J, Zhang Y X, Li G, Li M X. 2005. Retrospect of earthquake forecast and prospect (in Chinese). Rec Dev World Seismol, 5: 39–53
Zhang P Z, Molnar P, Burchfiel B C, Royden L, Wang Y P, Deng Q D, Song F M, Zhang W Q, Jiao D C. 1988. Bounds on the Holocene slip rate of the Haiyuan fault, north-central China. Quat Res, 30: 151–164
Zhang P Z, Min W, Deng Q D, Mao F Y. 2005. Paleoearthquake rupture behavior and recurrence of great earthquakes along the Haiyuan fault, northeastern China. Sci China Ser D-Earth Sci, 48: 364–375
Zhang P Z, Deng Q D, Zhang Z Q, Li H B. 2013. Active faults, earthquake hazards and associated geodynamic processes in continental China (in Chinese). Sci China Earth Sci, 43: 1607–1620
Zhao Y L, Qian F Y. 1994. Geoelectric precursors to strong earthquakes in China. Tectonophysics, 233: 99–113
Zheng W J, Zhang P Z, He W G, Yuan D Y, Shao Y X, Zheng D W, Ge W P, Min W. 2013. Transformation of displacement between strike-slip and crustal shortening in the northern margin of the Tibetan Plateau: Evidence from decadal GPS measurements and late Quaternary slip rates on faults. Tectonophysics, 584: 267–280
Zhou S Y. 2008. Seismicity simulation in western Sichuan of China based on the fault interactions and its implication on the estimation of the regional earthquake risk (in Chinese). Chin J Geophys, 51: 165–174
Zhu A Y, Zhang D N, Jiang C S. 2016. Numerical simulation of the segmentation of the stress state of the Anninghe-Zemuhe-Xiaojiang faults. Sci China Earth Sci, 59: 384–396
Zhu S B, Zhang P Z. 2013. FEM simulation of interseismic and coseismic deformation associated with the 2008 Wenchuan earthquake. Tectonophysics, 584: 64–80
Zilio L D, Van D Y, Gerya T V, Pranger C C. 2018. Seismic behaviour of mountain belts controlled by plate convergence rate. Earth Planet Sci Lett, 482: 81–92

(Responsible editor: Dinghui YANG)